

Higgs-boson phenomenology: a broad perspective

Laura Reina*

*Physics Department, Florida State University
77 Chieftan Way, 32306-4350 Tallahassee, FL - USA
E-mail: reina@hep.fsu.edu*

This talk reviews recent theoretical developments in Higgs-boson phenomenology and their impact on the Higgs-physics program of the Large Hadron Collider.

*7th Annual Conference on Large Hadron Collider Physics - LHCP2019
20-25 May, 2019
Puebla, Mexico*

*Speaker.

1. Overview

The understanding of the electroweak symmetry breaking (EWSB) is at the core of some of the main remaining open questions in particle physics and cosmology. The discovery of a Higgs boson at the Large Hadron Collider (LHC) has made this connection even more compelling and intriguing. In spite of the fact that the discovered Higgs boson seems to conform to the properties predicted by the Standard Model (SM), its nature is still very mysterious. The smallness of its mass seems to be due to unnatural fine-tuned cancellations. We do not know if it is part of a larger family of scalar fields as predicted by more complex mechanisms of EWSB. We have not even firmly established if this particle is elementary or composite. Answering these questions necessarily involves physics beyond the SM (BSM), and a broad Higgs phenomenology program could be one of the best portals to start its exploration. This is why Higgs physics has been at the core of the LHC physics program and will continue to be during its energy and luminosity upgrades.

After the discovery of a Higgs boson during Run 1 of the LHC, the main focus of Run 2 has been the measurement of its properties, in particular of its mass, width, and couplings. Deviations from the SM pattern of Higgs-boson couplings, as well as evidence for anomalies in the Higgs-boson width, could provide indirect evidence of new physics. Thanks to the number of events accumulated during Run 2, the LHC experiments have also been able to obtain statistically significant measurements of kinematic distributions from Higgs-boson production, and they have started investigating the effect of anomalous interactions on their shape. In parallel, direct searches have explored simple extensions of the Higgs sector of the SM, such as 2 Higgs Doublet Models (2HDM), models with extra scalar singlets, and a variety of other models with extended scalar sectors. In general, many such models admit a limit in which the properties of one of the scalars *align* with the ones of the SM Higgs boson, and could therefore provide a natural candidate for the SM-like Higgs boson discovered at the LHC. Indeed, current experimental constraints on 2HDM very much constrain them to such alignment regime, as illustrated in Fig. 1 for various types of 2HDM. As a plus, models with extended scalar sectors can provide candidates for dark matter, while models with multiple scalars can introduce additional sources of CP violation in the scalar sector and provide in this way one of the ingredients to explain baryogenesis. A broad range of models that could allow for exotic decays of the discovered Higgs boson have also been explored and bounds have been obtained both via direct searches and indirectly through measurements of the Higgs-boson width.¹

Not having found direct evidence of new particles, and not having measured any large deviations in the properties of the discovered Higgs boson from the SM predictions so far, we expect new physics to be sneaky and not likely to produce big deviations from SM predictions or unmistakable signals. Moving forward, we face two main challenges. On one hand we need to assess and provide the level of theoretical accuracy needed to meaningfully analyze current and future LHC data searching for small deviations, on the other hand we need to develop a successful strategy to interpret such data and in particular possible anomalies. I will discuss both aspects in the following sections.

¹ See summary talk by Jacobo Konigsberg as well as many contributions in the parallel sessions of this conference.

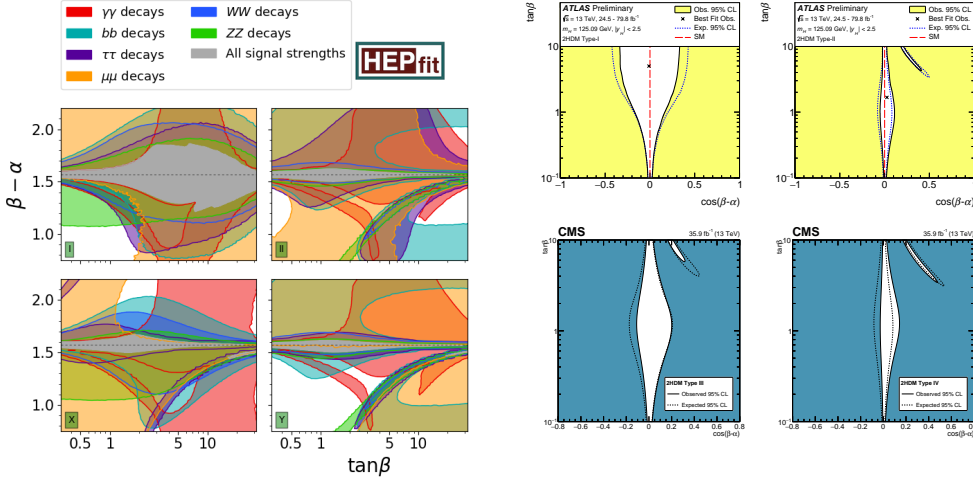


Figure 1: Experimental constraints on different types of 2HDM from the combined fit presented in Ref. [1] and from the most recent publications of the LHC experiments [2, 3].

2. Towards Higgs-boson precision physics

Precision physics can become a very powerful tool to constrain new physics when both theoretical predictions and experimental measurements reach a similar level of accuracy. On the theoretical side, competing with the accuracy of the LHC experiments is challenging but nevertheless possible since we have a predictive theory, the Standard Model, that allows us to calculate the observables measured in experiments within uncertainties that can be systematically improved. Indeed, the Higgs-boson discovery during Run 1 has offered a prominent example of synergy between the accuracy of experimental measurements and theoretical predictions [4, 5, 6, 7]. As part of the global effort that led to the Higgs-boson discovery, all Higgs-boson production and decay rates have been calculated including at least the first order of QCD and EW corrections for all the main production modes. Notably, today the leading production mode, gluon-gluon fusion ($gg \rightarrow H$), as well as $b\bar{b} \rightarrow H$, are known at $N^3\text{LO}$ in QCD [8, 9] and all production modes except the associated production with a $t\bar{t}$ pair are known at NNLO of QCD and NLO of EW corrections.² Similarly, several orders of QCD and EW corrections are known for all decay modes. The residual theoretical uncertainties on the fixed-order cross sections and branching ratios are for most modes reduced to only a few percent, the largest residual uncertainties from scale-dependence, α_s , and PDF being of the order of approximately 15-20% in the case of Higgs-boson production with heavy quarks (top and bottom).

Run 2 of the LHC has provided a first quite impressive test of the the Higgs-boson couplings and reported an overall consistency with the SM pattern. A snapshot of the most updated measurements is offered in Fig. 2 where the deviation from the SM Higgs-boson couplings to gauge bosons and fermions is presented in terms of overall rescaling factors $\kappa_i = g_i/g_i^{SM}$ [3, 2]. One can see that Higgs-boson couplings to gauge bosons have been measured at the 10-15% level, while Yukawa couplings to third generation fermions have been determined with 20-30% accuracy. Not shown in Fig. 2 is the measurements of the Higgs-boson self coupling (λ). In this case, first bounds have

²See talk by Bernhard Mistlberger at this conference.

been established from both double ($-5.2 \leq \kappa_\lambda \leq 12.1$) [10, 11] and single ($-3.2 \leq \kappa_\lambda \leq 11.9$) [12] Higgs production.

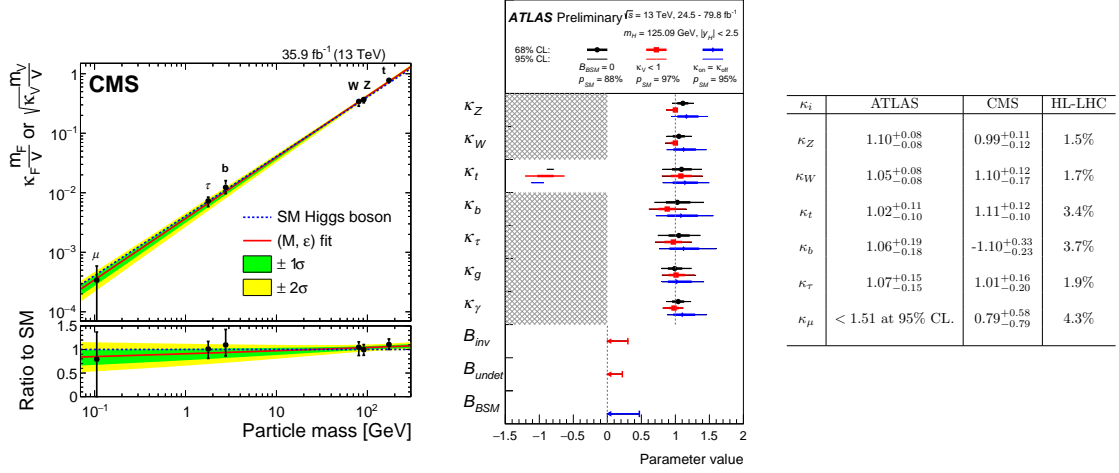


Figure 2: Summary of the fits for deviations in the Higgs-boson couplings to gauge bosons and fermions from both CMS [3] and ATLAS [2]. The r.h.s. table summarizes the corresponding results when no BSM contributions to Higgs-boson decays are assumed to exist and Higgs-boson vertices involving loops are resolved in terms of their SM content. The table also includes projections of the accuracy reachable at the HL-LHC with 3000 fb^{-1} per experiment [13].

If very accurate theoretical predictions of the total production cross sections have been crucial to establish the existence and the overall compatibility of the discovered Higgs boson with the SM, similar and higher level of accuracy for both total and differential cross sections will play an even more essential role in identifying signatures of new physics in the measurements of its couplings, including non-SM interactions induced by new physics beyond the LHC reach. New physics could affect the SM-like couplings of the Higgs boson, and could also introduce new *effective* couplings that arise at the electroweak scale when the exchange of very massive particles at high-energy induces new contact interactions. In both cases, new physics will cause ratios of measured couplings to the predicted SM couplings (the $\kappa_i = g_i/g_i^{SM}$ factors of Fig. 2) to deviate from unity. In the second case the shape of differential phase-space distributions should also be affected and the effects will be particularly enhanced in the tails of momentum, energy, and invariant-mass distributions.³ Controlling these scarcely populated regions is clearly experimentally challenging, but after Run 2 of the LHC we are fairly confident that it can be achieved. Still, given the established overall consistency of the SM, deviations will be small and only a very accurate prediction of total and differential rates for both signal and, in many cases, background processes is mandatory.

In fact, from a breakdown of the main sources of systematic errors affecting several Higgs-boson production measurements, we can see how theoretical uncertainties on the prediction of both signal and background are becoming one of the main entries in the overall uncertainty balance. As an example, in the l.h.s. plot of Fig. 3 (from Ref. [2]) we see the effect of different systematic uncertainties on the measurement of a global Higgs-boson signal strength (μ , to which all $\mu_{if} = \sigma_i \times BR_f / (\sigma_i \times BR_f)_{SM}$ have been set), presented in terms of the profiled likelihood ratio

³See talk by Dorival Gonçalves at this conference.

$\Lambda(\mu)$ (see [2] for details). The different curves represent the cases in which: 1) all systematic uncertainties are included (solid black line), 2) parameters describing theory uncertainties in background processes are fixed to their best-fit values (solid blue line), 3) the same procedure is also applied to theory uncertainties in the signal process (solid red line), and 4) to all systematic uncertainties, so that only statistical uncertainties remain (dotted black line). From the l.h.s. plot of Fig. 3, as well as the red-boxed entries in the table given in the r.h.s. of the same figure, we clearly see how the component of the systematic uncertainty coming from theory predictions and modeling of both signal and background is becoming a limiting factor in achieving better experimental accuracies. In these estimates, the theory component includes uncertainties due to missing higher-order perturbative QCD and electroweak corrections in the MC simulation, uncertainties in PDF and α_s , the treatment of the underlying events, the matching between the hard-scattering process and the parton shower, the choice of hadronization models, and branching fraction uncertainties. In general the residual dominant uncertainties arise from the theory modeling of the signal and background processes in simulations. In the following we will review the most recent progress made towards improving the accuracy of theoretical predictions, with attention to the fact that such progress may concern different aspects of the theoretical predictions for different processes.

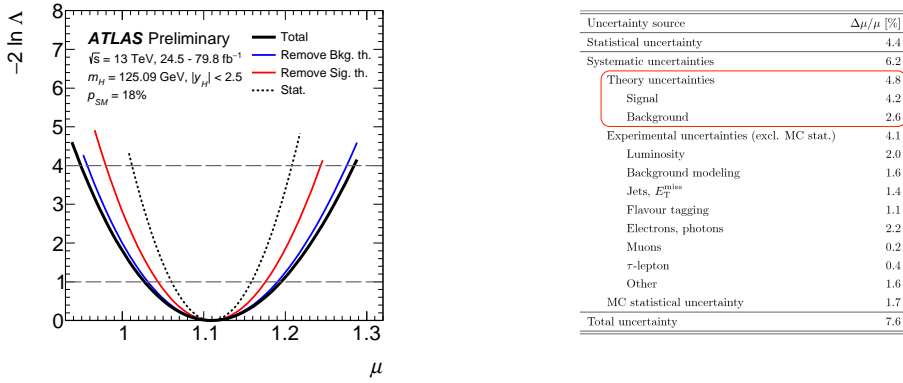


Figure 3: Variations of $2 \ln \Lambda(\mu)$ as a function of the global Higgs-boson signal strength μ (l.h.s.) and breakdown of the corresponding systematic uncertainty from different sources (r.h.s.). See text for details. From Ref.[2].

Indeed, understanding the impact of higher-order corrections and the residual theoretical uncertainty on kinematic distributions can often be a process-dependent task, based on understanding what choices can improve the QCD and EW perturbative calculation of a given process. Examples are the choice of the central value for renormalization and factorization scales, which can be very different in nature and value process by process, or the choice to include partial higher-order corrections if they help to stabilize the contribution of certain dominant subprocesses. On the other hand, predicting distributions with satisfactory theoretical accuracy in general involves further challenges, independently of the process considered. To start with, matching experimental distributions often requires more exclusive final states, and providing higher-order corrections for such more exclusive states often goes beyond the difficulty of providing the same order of corrections for the corresponding inclusive processes. Moreover, a realistic description of exclusive collider events

requires matching fixed-order calculations to parton-shower event generators and understanding how to estimate the consequent residual level of theoretical uncertainty.⁴ Finally, predicting distributions requires validating the theoretical description of a given process in all kinematical regions of interest. For instance, total cross sections can be marginally affected by deviations in the tail of distributions, and we can forgo being very accurate in these regions if the goal is just measuring total rates. But if we want e.g. to detect deviations in the shape of distributions at high p_T , we need to be sure of the validity of our calculation in that region. So, accurately predicting distributions may require revisiting theoretical calculations previously used for total rates only.⁵

In this context, the prediction of the Higgs-boson transverse-momentum (p_T^H) distribution including higher-orders of QCD corrections plays indeed a special role in testing and constraining multiple aspects of Higgs-boson physics. On one hand, knowing the p_T distribution of a Higgs boson produced with one or more jets can be very effective in enhancing the signal-to-background ratio in several channels, since signatures with associated jets can allow to disentangle different production mechanisms or use a broader spectrum of decay signatures. At the same time, the high- and low- p_T regions of this distribution can provide unique handles on some Higgs-boson Yukawa couplings. More specifically, the high p_T region can resolve the dependence on m_t , and test the relation between the top-quark Yukawa coupling and the Hgg coupling, as well as any anomalous Higgs interaction that can affect high-energy tails of distributions. On the other hand, the low- p_T^H region, being sensitive to light-quark mass effects (m_b and, possibly, m_c), could provide information on the Higgs-boson couplings to light-quarks.

Building upon the NNLO QCD calculation of $H + 1j$ [14, 15], a lot of recent activity has been focusing on improving the theoretical description of the p_T^H distribution in both the high and low p_T regions. These regions are particularly affected by higher order corrections, either because, in the case of high p_T , additional hard QCD radiation, hence high-jet multiplicity, pushes the Higgs-boson to higher p_T , or because, in the case of low p_T , the resummation of soft QCD radiation is crucial to correctly modelling the low- p_T regions of the spectrum. In both cases, higher-order QCD corrections and finite quark-mass effects can be particularly relevant. In the high p_T region the validity of using the $m_t \rightarrow \infty$ limit (a.k.a. Higgs Effective Theory, or HEFT), where the ggH top-loop induced interaction is reduced to a pointlike ggH contact interaction, has been assessed by two different groups who have calculated the p_T^H distribution of $H + j$ at NLO in QCD including finite m_t effects exactly [17] or retaining the leading terms in an m_t^2/p_T^2 expansion with $m_t \gg m_H$ (i.e. setting de facto $m_H = 0$) [16]. Results from both studies are collected in Fig. 4. Clearly the HEFT approach fails to describe the shape of the p_T^H distribution above 300-400 GeV, where finite top-quark mass effects are not negligible and the accuracy of theoretical prediction strongly relies not only on the perturbative order but also on the capability of including such effects. Both calculations also confirm that, in spite of the fact that the HEFT only poorly approximates the shape of the spectrum at high p_T , K -factors in the HEFT and in the full theory behave in a very similar way above 200 GeV, hence suggesting that a good approximation of the full NNLO distributions could be obtained by rescaling the corresponding NLO distributions (with full m_t dependence) by the the NNLO HEFT K factor.

⁴See talk by Emanuele Re at this conference.

⁵See talk by Kirill Melnikov at this conference.

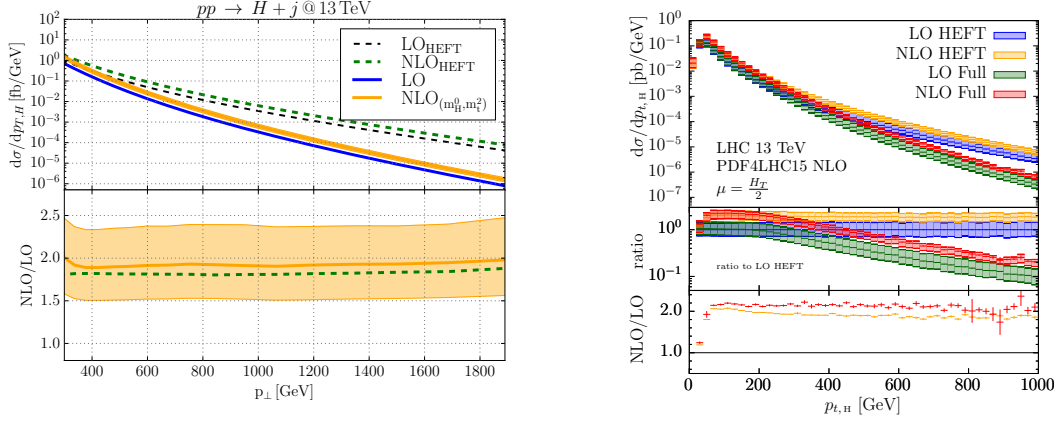


Figure 4: Transverse momentum distribution of the Higgs boson at the LHC with $\sqrt{s} = 13$. Both plots illustrate the comparison between LO and NLO predictions in the full SM and in the infinite top-mass approximation (HEFT). See text for details. L.H.S. from Ref. [16]. R.H.S.: from Ref. [17].

At the opposite end of the spectrum, in the low- p_T^H region, Higgs-boson production is enhanced by logarithms of m_H/p_T arising from multiple soft gluon radiation. Working in the $m_t \rightarrow \infty$ approximation, i.e. for a pointlike ggH interaction, the accuracy of the resummation of such logarithmic corrections has been improved over the years and $N^3LL+NNLO$ results have been presented for the first time in Ref. [18], from where the l.h.s. plot of Fig. 5 has been extracted. As often the case, controlling large logarithmic corrections beyond the NLO and NNLO fixed orders reduces their sharp impact in the peak region (around p_T^H of 15 GeV) and stabilizes the shape of the spectrum with respect to higher-order corrections. Based on this very important result, more recently the impact of light-quark corrections (namely b quarks) in the $m_b \leq p_T \leq m_H$ region has been investigated at NNLL+NLO QCD, including both top- and bottom-quark contributions. Indeed, the bottom-quark Yukawa coupling has a non-negligible impact on the total cross section through the interference of bottom- and top-quark contributions, and sensibly affects the shape of the p_T^H spectrum in the low- p_T region, as illustrated in the r.h.s. plot of Fig. 5. The residual theoretical uncertainty is estimated in Ref. [19] to be of the order of 15-20% and mainly dominated by the fixed-order NLO top contribution. This could therefore be improved in the future, reducing the error on both total and differential cross sections to a level that would allow to extract information on the bottom-quark Yukawa coupling for which the direct extraction from associated production of a Higgs boson with bottom quarks is particularly challenging at the LHC.

If the inclusive production of a Higgs-boson, being dominated by $gg \rightarrow H$ via an internal loop of top quarks, indirectly measures the top-quark Yukawa coupling, the associated production of a Higgs-boson with a $t\bar{t}$ pair gives the main direct access to such coupling. The accuracy of the experimental measurement is currently limited by the theoretical uncertainty on the prediction of its most important backgrounds, namely $t\bar{t} + b$ jets and $t\bar{t}V$ with $V = W/Z$ decaying leptonically. Ongoing dedicated studies [7, 20, 21] have recently clarified several aspects of the $t\bar{t} + b$ jets background and showed the need for a better understanding of the interplay between higher-order fixed-order predictions (currently available at NLO QCD+EW) and parton-shower generators. In

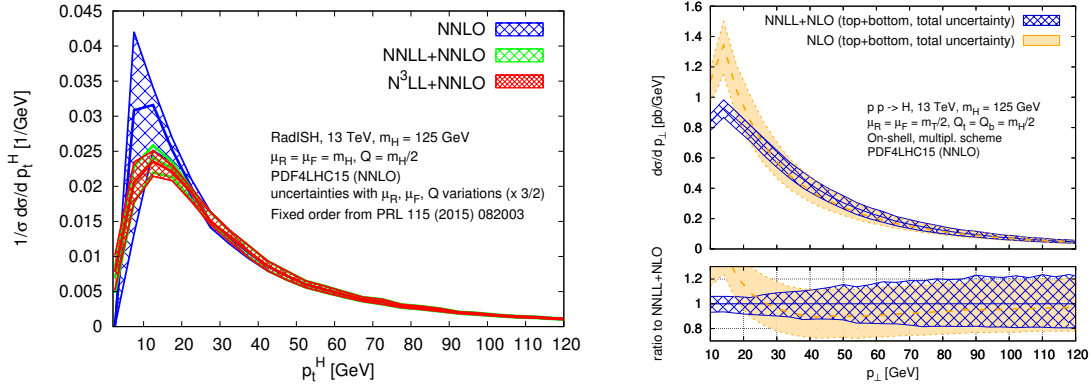


Figure 5: Transverse momentum distribution of the Higgs boson at the LHC with $\sqrt{s} = 13$. L.H.S.: Comparison among the matched normalised distributions at N³LL+NNLO, NNLL+NNLO, and NNLO, from Ref. [18]. R.H.S.: comparison between the full matched distribution at NNLL+NLO and NLO, from Ref. [19].

this case adding higher-orders of quantum corrections is not an immediate priority, contrary to the case of the p_T^H distributions we discussed earlier. Of particular interest in understanding the relevance of different regimes (e.g. hard scattering versus parton showering) and different processes (e.g. b jets produced from initial-state or final-state gluon radiation) are the recent calculation of $t\bar{t}b\bar{b} + j$ at NLO in QCD [21], and the development of a new merging algorithm (*Fusing*) where, building upon the established merging algorithms for multi-jet matrix elements and parton showers, a new technique to merge the NLO QCD massive $t\bar{t} + b\bar{b}$ matrix elements into the $t\bar{t} + jj$ has been proposed [22]. Furthermore, studying the dynamics of one extra jet emission at higher order in QCD has allowed to identify effects induced by the parton-shower [21] and develop strategies to compensate for them.⁶ Different NLO PS frameworks, based on different shower and matching methods, can now be shown to provide consistent predictions,⁷ which in turn will allow to reduce the corresponding systematic errors from theoretical modelling. At the same time the possibility of modelling the production of b jets based on the hard scattering matrix element or gluon splitting ($g \rightarrow b\bar{b}$) in different regimes has given very promising results in the case of $Z + b$ jets production and could potentially bring the modelling of b - and light-jet distributions in $t\bar{t}b\bar{b}$ production under better control [23]. As far as $t\bar{t}V$ with $V = W/Z$ decaying to leptons goes, the on-shell production is known at NLO of QCD+EW corrections [24, 25], and dedicated experimental measurements by both ATLAS and CMS confirm the SM predictions within the still non-negligible uncertainties. At the same time, some disagreement is emerging when $t\bar{t}W$ is considered in the context of $t\bar{t}H$ analyses, where, apparently, a preliminary clear excess with respect to the SM is reported [26]. To understand the nature of the issue theoretical predictions will have to be revisited, at least to the extent of controlling W and top-quark decays and their kinematics at the best of the available tools.

The final fundamental step in the Higgs-boson precision program will be to validate the pattern of EWSB as realized by the scalar potential of the SM. In this context, a crucial constraint will come from a measurement of the Higgs-boson self-coupling (λ). In particular, Higgs-boson pair

⁶See talk by Tomas Jezo at this conference.

⁷See ongoing studies within the $t\bar{t}H/tH$ subgroup of the Higgs XS Working Group.

production has received a lot of experimental and theoretical attention as it gives access to the triple Higgs-boson self coupling in a variety of channels identified by the decay products of the Higgs-boson pair. The theoretical prediction for such process is dominated by gg fusion via a loop of top quarks and the state-of-the-art calculations of the exact top-mass dependence for the NLO QCD total cross section and the M_{HH} invariant mass distribution have shown effects of 10-30% with respect to what had been previously calculated in different approximations, including the HEFT, and have reduced the theoretical uncertainty on the (approximated) NNLO cross section to about 5% [27, 28]. At the same time, the Higgs-boson self-coupling could be constrained through quantum loop effects on EW observables (e.g. M_W, \dots) and Higgs-boson decays (e.g. $H \rightarrow WW, ZZ$), as well as single Higgs-boson production. Ref. [29] found a bound of $\kappa_\lambda > -14.3$ on $\kappa_\lambda = \lambda_3/\lambda_3^{SM}$ (where λ_3 denotes the value of λ appearing in the triple Higgs-boson self-coupling), while Refs. [30, 31] constrain κ_λ to be in the range $-14 < \kappa_\lambda < 18$ from loop-effects on EW precision observables. Both avenues have been explored experimentally and have provided bounds in full compatibility with these theoretical estimates, as discussed earlier in this section.

3. Testing the SM consistency including EW and Higgs data

Direct searches of new physics will always be the core of the physics program of any collider. As the discovery of the Higgs boson has nailed a pin on the map of all possible BSM theories, new discoveries would unquestionably exclude families of BSM models in favor of others. At the same time, building on the increasing precision being reached in both experimental measurements and theoretical predictions, a very intense program of constraining new physics via a combined fitting of EW precision observables (EWPO) and Higgs-boson observables have been developed.

In either case the interpretation of anomalies, in e.g. the high-energy tail of Higgs-boson distributions or in global EW precision fits of the SM, could be approached within a specific model or in terms of effective interactions that are induced at the EW scale by more general classes of high-energy theories. Examples of model-specific searches have been given in Sec. 1 and many more have been presented in the course of this meeting. On the other hand, a more model-independent approach has been focusing on the so-called SM effective field theory (SMEFT), where the SM Lagrangian is extended by operators of dimension 6 and higher:

$$\mathcal{L}_{\text{eff}} = \mathcal{L}_{\text{SM}} + \mathcal{L}_{\text{light NP}} + \sum_{d>4} \frac{1}{\Lambda^{d-4}} \mathcal{L}_d, \quad \text{with } \mathcal{L}_d = \sum_i C_i \mathcal{O}_i, \quad [\mathcal{O}_i] = d. \quad (3.1)$$

Studies so far have focused on considering mainly dimension-6 operators expressed in terms of SM fields, i.e. assuming only one doublet of complex scalar fields in a linearly realized spontaneous symmetry breaking. Thanks to the increased statistics of Run 2, enough Higgs-boson measurements (both in the form of total and differential cross sections) have become available to allow for a combined fit of EWPO and Higgs-boson observables in terms of a reduced basis of dimension-6 operators that assumes flavour universality and CP conservation. Examples of such fits have been presented by several groups [32, 33, 34] that also tested the validity of including only dimension-6 operators by probing the sensitivity of the fit results to a linear versus a quadratic expansion of the theoretical predictions in the EFT coefficients [33, 34].⁸ Given the special role played by the top-

⁸See talk by Emma Slade's at this conference.

quark in Higgs-boson production, more recent studies have lifted flavour universality for the third generation of quarks, and used that to probe the SM degeneracy between Higgs-boson couplings to gluons and top quarks (see in particular [35, 36]).

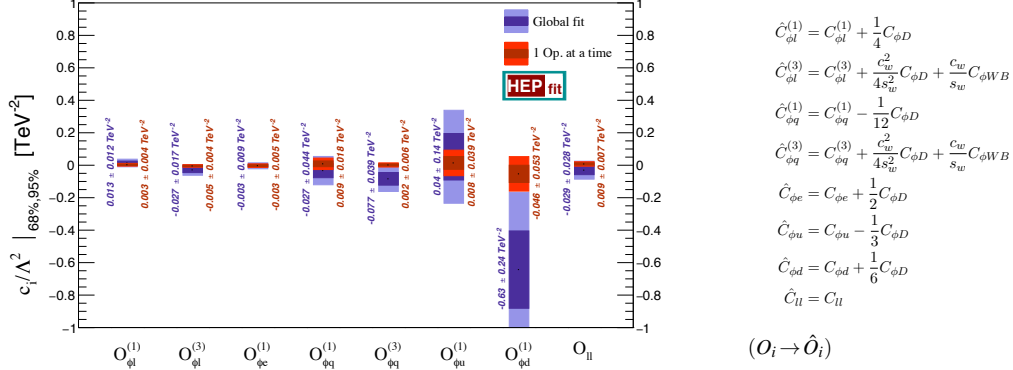


Figure 6: Constraints on the eight linear combinations of coefficients of dimension-6 operators entering in EWPO. The blue bands represent the simultaneous fit to all operators in a given set, the red bands represent the fit to one operator at a time. Dark and light shadows indicate 1σ and 2σ intervals.

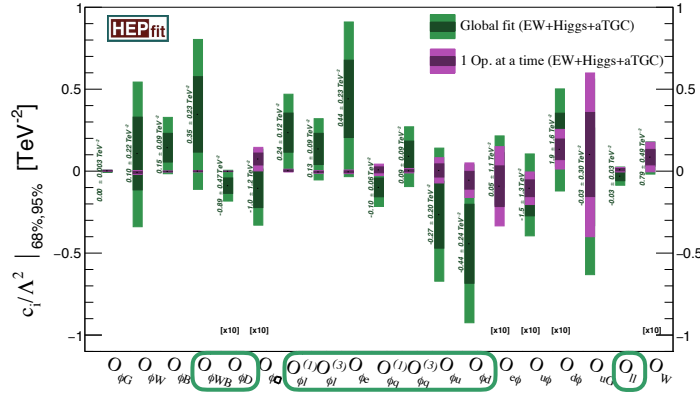


Figure 7: Constraints on the coefficients of dimension-6 operators entering in both EWPO and Higgs-boson observables. The green bands represent the simultaneous fit to all operators in a given set, the purple bands represent the fit to one operator at a time. Dark and light shadows indicate 1σ and 2σ intervals.

For the purpose of illustration of these studies that should all be considered as very exploratory, we collect in Figs. 6, 7, and 8 results obtained by the HEPFIT collaboration [37]. They are expressed in terms of coefficients of dimension 6 operators in the so-called Warsaw basis [38], and involve only operators that enters either in EWPO observables or in Higgs-boson signal-strength predictions. Bounds are given for the ratios C_i/Λ^2 (see Eq. 3.1), and can therefore be interpreted either as bound on the C_i coefficients for a given Λ or translated into lower bound on Λ for given values of the coefficients. Typically finding large coefficients C_i would not be compatible with truncating the SMEFT expansion to dimension 6 only. At the same time, too low bounds on Λ could signal some tension in justifying an EFT approach. Only ten operators contribute to EWPO and only eight independent linear combinations (see Fig. 6) can be constrained by an EW global

fit. The plot in Fig. 6 shows results for a global fit of these eight combinations (blue bands). For comparison results obtained by inserting only one operator at a time are presented (red bands). A part from the obvious fact that errors are smaller when fitting just one operator at a time, we should also observe that from the difference in the bounds obtained on some coefficients in the two cases, we can infer the existence of large correlations. At the same time, the data now available from Run 2 and our understanding of the underlying theory are such that ignoring correlations is becoming unrealistic and should probably not be considered if not for comparison, as an indication of where correlations will play a major/minor role. In the plot of Fig. 7 the fit is extended to include also Higgs-boson observables (signal strength) and triple-gauge coupling data. All ten operators that enter EWPO can now be separately fit (see operators circled in green) since their degeneracy is lifted, and new operators are added as needed to describe the Higgs-boson observables included in the fit. For operators that contribute to both EWPO and Higgs-boson observables, it is still true that their coefficients are more tightly constrained by EWPO. The difference between individual and global constraints confirms that large correlations exist and global fits are to be preferred. For scales $\Lambda = 1$ TeV (or larger) most coefficients are quite small, and only a fit that also consistently included quadratic terms in all the C_i could probably test the need for higher dimension operators. Considering the effect of these operators on differential distributions [39, 40] as well as connecting to the constraints induced by flavour-physics observables below the electroweak scale [41] will provide more and more constraining information that will help extracting more definite information on NP from the SMEFT global fits.

Coefficient	95% prob. range C_i/Λ^2 [TeV ⁻²]	95% prob. lower bound on Λ [TeV] ($ C_i = 1$)
$C_{\phi G}$	[-0.00029, 0.0059]	13.5
$C_{\phi W}$	[-0.019, 0.0040]	7.63
$C_{\phi B}$	[-0.0051, 0.0011]	14.7
$C_{\phi WB}$	[-0.0045, 0.0038]	15.7
$C_{\phi D}$	[-0.027, 0.00092]	6.38
$C_{\phi \square}$	[0.015, 1.4]	0.85
$C_{\phi L}^{(1)}$	[-0.0052, 0.012]	9.81
$C_{\phi L}^{(3)}$	[-0.013, 0.0030]	9.46
$C_{\phi e}^{(1)}$	[-0.015, 0.0070]	9.14
$C_{\phi e}^{(3)}$	[-0.027, 0.043]	5.13
$C_{\phi q}^{(3)}$	[-0.0111, 0.015]	8.71
$C_{\phi u}$	[-0.072, 0.082]	3.59
$C_{\phi d}$	[-0.16, 0.050]	2.72
$C_{\phi \phi}$	[-0.034, 0.015]	5.97
$C_{u\phi}$	[-2.0, -0.050]	0.74
$C_{d\phi}$	[0.0031, 0.061]	4.18
C_{LL}	[-0.0048, 0.022]	7.11

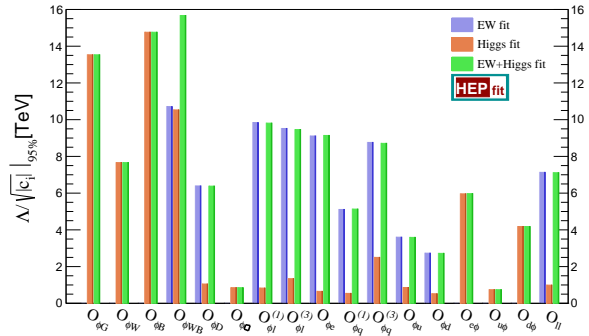


Figure 8: Lower bounds on the scale of new physics Λ from a fit to the dimension-6 coefficients entering in EW+Higgs observables fitting one operator at a time. The different colors represent the cases in which only EW, only Higgs, or both EW and Higgs constraints are considered.

Finally, in Fig. 8 the effects of the fit (this time with one operator at a time just for illustration purposes) on both coefficients and Λ are shown side by side, together with the effect of EWPO, Higgs-observables, and both combined, on each coefficient. It is interesting to note that achieving higher precision in the fit (which depends on both theoretical and experimental inputs) would allow for a more constrained determination of the EFT coefficients and in turn translate into higher reach in the scale Λ that can be probed. A 10% increase in precision on the coefficients could give access to scales as high as 100 TeV. Projections of the reach of global fit at future colliders have been the topic of dedicated sessions at this meeting and a very comprehensive study can be found in Ref. [42] as part of the development of the European Strategy for Particle Physics.

4. Outlook

After the discovery of the Higgs boson during Run I of the LHC, a major effort to develop a full-fledged precision program to measure its couplings has been growing. Indirect evidence of new physics from Higgs-boson and EW precision measurements could come from the synergy between accurate theoretical prediction, a systematic approach to the study of new effective interactions, and the intuition and experience of many years of beyond SM searches. Increasing the precision of input parameters could allow to test higher scales of new physics and provide very valuable information for both present and future colliders. Direct evidence of new physics could clearly boost this process, as the discovery of a Higgs-boson has prompted and guided us in this new era of LHC physics.

References

- [1] D. Chowdhury and O. Eberhardt, *Update of Global Two-Higgs-Doublet Model Fits*, *JHEP* **05** (2018) 161, [[arXiv:1711.02095](#)].
- [2] **ATLAS Collaboration**, G. Aad et al., *Combined measurements of Higgs boson production and decay using up to 80 fb^{-1} of proton–proton collision data at $\sqrt{s} = 13\text{ TeV}$ collected with the ATLAS experiment*, [arXiv:1909.02845](#).
- [3] **CMS Collaboration**, A. M. Sirunyan et al., *Combined measurements of Higgs boson couplings in proton-proton collisions at $\sqrt{s} = 13\text{ TeV}$* , Submitted to: *Eur. Phys. J.* (2018) [[arXiv:1809.10733](#)].
- [4] **LHC Higgs Cross Section Working Group Collaboration**, S. Dittmaier et al., *Handbook of LHC Higgs Cross Sections: 1. Inclusive Observables*, [arXiv:1101.0593](#).
- [5] **LHC Higgs Cross Section Working Group Collaboration**, S. Dittmaier et al., *Handbook of LHC Higgs Cross Sections: 2. Differential Distributions*, [arXiv:1201.3084](#).
- [6] **LHC Higgs Cross Section Working Group Collaboration**, J. R. Andersen et al., *Handbook of LHC Higgs Cross Sections: 3. Higgs Properties*, [arXiv:1307.1347](#).
- [7] **LHC Higgs Cross Section Working Group Collaboration**, D. de Florian et al., *Handbook of LHC Higgs Cross Sections: 4. Deciphering the Nature of the Higgs Sector*, [arXiv:1610.07922](#).
- [8] C. Anastasiou, C. Duhr, F. Dulat, E. Furlan, T. Gehrmann, F. Herzog, A. Lazopoulos, and B. Mistlberger, *High precision determination of the gluon fusion Higgs boson cross-section at the LHC*, *JHEP* **05** (2016) 058, [[arXiv:1602.00695](#)].
- [9] C. Duhr, F. Dulat, and B. Mistlberger, *Higgs production in bottom-quark fusion to third order in the strong coupling*, [arXiv:1904.09990](#).
- [10] **CMS Collaboration**, A. M. Sirunyan et al., *Combination of searches for Higgs boson pair production in proton-proton collisions at $\sqrt{s} = 13\text{ TeV}$* , *Phys. Rev. Lett.* **122** (2019), no. 12 121803, [[arXiv:1811.09689](#)].
- [11] **ATLAS Collaboration**, G. Aad et al., *Combination of searches for Higgs boson pairs in pp collisions at $\sqrt{s} = 13\text{ TeV}$ with the ATLAS detector*, [arXiv:1906.02025](#).
- [12] **ATLAS Collaboration** Collaboration, *Constraint of the Higgs boson self-coupling from Higgs boson differential production and decay measurements*, Tech. Rep. ATL-PHYS-PUB-2019-009, CERN, Geneva, Mar, 2019.

- [13] **Physics of the HL-LHC Working Group** Collaboration, M. Cepeda et al., *Higgs Physics at the HL-LHC and HE-LHC*, [arXiv:1902.00134](#).
- [14] X. Chen, T. Gehrmann, E. W. N. Glover, and M. Jaquier, *Precise QCD predictions for the production of Higgs + jet final states*, *Phys. Lett.* **B740** (2015) 147–150, [[arXiv:1408.5325](#)].
- [15] R. Boughezal, F. Caola, K. Melnikov, F. Petriello, and M. Schulze, *Higgs boson production in association with a jet at next-to-next-to-leading order*, *Phys. Rev. Lett.* **115** (2015), no. 8 082003, [[arXiv:1504.07922](#)].
- [16] J. M. Lindert, K. Kudashkin, K. Melnikov, and C. Wever, *Higgs bosons with large transverse momentum at the LHC*, *Phys. Lett.* **B782** (2018) 210–214, [[arXiv:1801.08226](#)].
- [17] S. P. Jones, M. Kerner, and G. Luisoni, *Next-to-Leading-Order QCD Corrections to Higgs Boson Plus Jet Production with Full Top-Quark Mass Dependence*, *Phys. Rev. Lett.* **120** (2018), no. 16 162001, [[arXiv:1802.00349](#)].
- [18] W. Bizon, P. F. Monni, E. Re, L. Rottoli, and P. Torrielli, *Momentum-space resummation for transverse observables and the Higgs p_{\perp} at $N^3LL+NNLO$* , *JHEP* **02** (2018) 108, [[arXiv:1705.09127](#)].
- [19] F. Caola, J. M. Lindert, K. Melnikov, P. F. Monni, L. Tancredi, and C. Wever, *Bottom-quark effects in Higgs production at intermediate transverse momentum*, *JHEP* **09** (2018) 035, [[arXiv:1804.07632](#)].
- [20] T. Ježo, J. M. Lindert, N. Moretti, and S. Pozzorini, *New NLOPS predictions for $t\bar{t} + b$ -jet production at the LHC*, *Eur. Phys. J.* **C78** (2018), no. 6 502, [[arXiv:1802.00426](#)].
- [21] F. Buccioni, S. Kallweit, S. Pozzorini, and M. F. Zoller, *NLO QCD predictions for $t\bar{t}b\bar{b}$ production in association with a light jet at the LHC*, [arXiv:1907.13624](#).
- [22] S. Höche, J. Krause, and F. Siegert, *Multijet Merging in a Variable Flavor Number Scheme*, *Phys. Rev.* **D100** (2019), no. 1 014011, [[arXiv:1904.09382](#)].
- [23] G. Ridolfi, M. Ubiali, and M. Zaro, *A fragmentation-based study of heavy quark production*, [arXiv:1911.01975](#).
- [24] S. Frixione, V. Hirschi, D. Pagani, H. S. Shao, and M. Zaro, *Electroweak and QCD corrections to top-pair hadroproduction in association with heavy bosons*, *JHEP* **06** (2015) 184, [[arXiv:1504.03446](#)].
- [25] R. Frederix, D. Pagani, and M. Zaro, *Large NLO corrections in $t\bar{t}W^{\pm}$ and $t\bar{t}t$ hadroproduction from supposedly subleading EW contributions*, *JHEP* **02** (2018) 031, [[arXiv:1711.02116](#)].
- [26] **ATLAS** Collaboration, T. A. collaboration, *Analysis of $t\bar{t}H$ and $t\bar{t}W$ production in multilepton final states with the ATLAS detector*, .
- [27] S. Borowka, N. Greiner, G. Heinrich, S. P. Jones, M. Kerner, J. Schlenk, U. Schubert, and T. Zirke, *Higgs Boson Pair Production in Gluon Fusion at Next-to-Leading Order with Full Top-Quark Mass Dependence*, *Phys. Rev. Lett.* **117** (2016), no. 1 012001, [[arXiv:1604.06447](#)]. [Erratum: *Phys. Rev. Lett.* 117, no. 7, 079901 (2016)].
- [28] M. Grazzini, G. Heinrich, S. Jones, S. Kallweit, M. Kerner, J. M. Lindert, and J. Mazitelli, *Higgs boson pair production at NNLO with top quark mass effects*, *JHEP* **05** (2018) 059, [[arXiv:1803.02463](#)].
- [29] G. Degrossi, P. P. Giardino, F. Maltoni, and D. Pagani, *Probing the Higgs self coupling via single Higgs production at the LHC*, *JHEP* **12** (2016) 080, [[arXiv:1607.04251](#)].

- [30] G. Degrandi, M. Fedele, and P. P. Giardino, *Constraints on the trilinear Higgs self coupling from precision observables*, *JHEP* **04** (2017) 155, [[arXiv:1702.01737](#)].
- [31] G. D. Kribs, A. Maier, H. Rzehak, M. Spannowsky, and P. Waite, *Electroweak oblique parameters as a probe of the trilinear Higgs boson self-interaction*, *Phys. Rev.* **D95** (2017), no. 9 093004, [[arXiv:1702.07678](#)].
- [32] J. de Blas, M. Ciuchini, E. Franco, S. Mishima, M. Pierini, L. Reina, and L. Silvestrini, *The Global Electroweak and Higgs Fits in the LHC era*, *PoS EPS-HEP2017* (2017) 467, [[arXiv:1710.05402](#)].
- [33] J. Ellis, C. W. Murphy, V. Sanz, and T. You, *Updated Global SMEFT Fit to Higgs, Diboson and Electroweak Data*, *JHEP* **06** (2018) 146, [[arXiv:1803.03252](#)].
- [34] E. da Silva Almeida, A. Alves, N. Rosa Agostinho, O. J. P. Éboli, and M. Gonzalez-Garcia, *Electroweak Sector Under Scrutiny: A Combined Analysis of LHC and Electroweak Precision Data*, *Phys. Rev.* **D99** (2019), no. 3 033001, [[arXiv:1812.01009](#)].
- [35] F. Maltoni, E. Vryonidou, and C. Zhang, *Higgs production in association with a top-antitop pair in the Standard Model Effective Field Theory at NLO in QCD*, *JHEP* **10** (2016) 123, [[arXiv:1607.05330](#)].
- [36] A. Azatov, C. Grojean, A. Paul, and E. Salvioni, *Resolving gluon fusion loops at current and future hadron colliders*, *JHEP* **09** (2016) 123, [[arXiv:1608.00977](#)].
- [37] J. de Blas et al., *HEPfit: a Code for the Combination of Indirect and Direct Constraints on High Energy Physics Models*, [arXiv:1910.14012](#).
- [38] B. Grzadkowski, M. Iskrzynski, M. Misiak, and J. Rosiek, *Dimension-Six Terms in the Standard Model Lagrangian*, *JHEP* **10** (2010) 085, [[arXiv:1008.4884](#)].
- [39] C. Degrande, B. Fuks, K. Mawatari, K. Mimasu, and V. Sanz, *Electroweak Higgs boson production in the standard model effective field theory beyond leading order in QCD*, *Eur. Phys. J.* **C77** (2017), no. 4 262, [[arXiv:1609.04833](#)].
- [40] M. Grazzini, A. Ilnicka, M. Spira, and M. Wiesemann, *Modeling BSM effects on the Higgs transverse-momentum spectrum in an EFT approach*, *JHEP* **03** (2017) 115, [[arXiv:1612.00283](#)].
- [41] L. Silvestrini and M. Valli, *Model-independent Bounds on the Standard Model Effective Theory from Flavour Physics*, [arXiv:1812.10913](#).
- [42] J. de Blas et al., *Higgs Boson Studies at Future Particle Colliders*, [arXiv:1905.03764](#).